2026 IEEE International Conference on Robotics and Automation (ICRA 2026)
June 1-5, 2026. Vienna, Austria

Identification and Reduction of Fat Shadows in Obese Patients using Robotic Echocardiography

Tomoshige Hashimoto, Soma Tsukamoto, Yuuki Shida, and Hiroyasu Iwata, *Member, IEEE*

***Abstract*— The present study proposes a method to identify fat and lung shadows and reduce fat shadows in obese patients to obtain clear ultrasound (US) images. The shadow identification method focuses on the difference between the luminance value of the shadow and the direction of image loss caused by the degree of reflection and absorption of US waves in fat and lungs, thereby registering the degree of image blurring caused by each shadow. The method for reducing fat shadows was based on preliminary experiments to derive the appropriate probe pressing pressure for the patient's BMI, enabling the acquisition of US images with fewer fat shadows while relieving the patient from feeling pressure. Verification tests were conducted using the proposed method. With regard to the shadow identification method, it was possible to detect fat shadows and lung shadows with an accuracy of 92.7% and 96.8% of the F-measure, respectively. The introduction of the shadow reduction method increased the number and range of mitral valve detections. These results underline the usefulness of the proposed method.**

I. Introduction

Cardiovascular diseases are the world's leading cause of death, with 17.9 million people dying of heart disease in 2019 [1]. Heart disease is a progressive disease, and early detection and treatment can reduce the mortality rate [2]. As a result, periodic health checkups using echocardiography have been attracting significant attention. Echocardiography is a noninvasive and highly accurate diagnostic method that is widely used for the diagnosis of the following three main causes of heart failure, a condition that has the highest mortality rate among all cardiac diseases: myocardial infarction, valvular heart disease, and cardiac hypertrophy. Ultrasonography, including transthoracic echocardiography, is a challenging examination. This is because the structure of the heart is complex, and there are individual variations in the shape and position of the patient's heart. Then, it is necessary to adopt a tailored approach for each individual during the examination. It is imperative for physicians and technologists to have a high level of skills and experience, which may also help to explain the manpower shortage noted in this field.

To solve these problems, previous studies proposed several assistive technologies for ultrasonographic examinations using robots [3]–[15]. However, there is a limited number of studies on the automation of echocardiographic examinations by robots. Nonetheless, the authors have proposed a posture angle control system to realize a seated echocardiography robot (see **Fig. 1**) and an automatic robot search method for the parasternal long axis view, which is one of the basic views required for diagnosis of cardiac disease [16], [17].

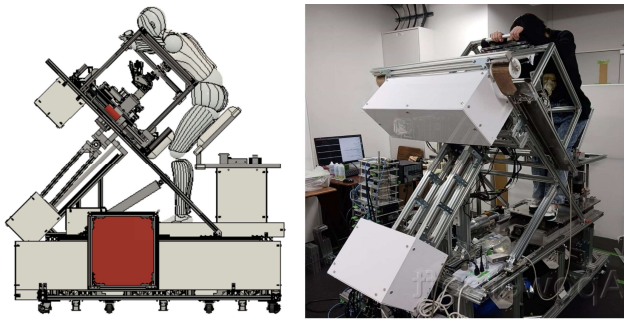

Fig.1. Seated-style echocardiography robot

(a) (b)

Fig.2. Effect of fat and lung shadows on echocardiographic US images
(a) Normal image (b) Image with fat shadows

In contrast, in obese patients, shadows caused by subcutaneous fat and lungs reduce the clarity of US images, which in turn decreases the accuracy of the automatic search (see **Fig. 2**). Both subcutaneous fat and lungs absorb and reflect US waves, making it difficult for US waves to penetrate deep into these tissues and observe the heart, which resides deep within them. The effect of subcutaneous fat can be resolved by pressing the probe hard against the body, while the effect of the lungs can be resolved by instructing patients to exhale air. However, in the medical field, adjustment of the

*This research was supported by the NSK Foundation for Advancement of Mechatronics and the Institute for Mechanical Engineering Frontiers.

T. Hashimoto, S. Tsukamoto, and Y. Shida is with the Graduate School of Creative Science and Engineering, Waseda University, Tokyo 169-8050, Japan (e-mail:thaumatrope@suou.waseda.jp)

H. Iwata is with the Faculty of Science and Engineering, Waseda University, Tokyo 169-8050, Japan (e-mail: jubi@waseda.jp).

degree of pressing the probe and the amount of air exhalation is subjective and has thus not been quantitatively analyzed. Furthermore, although these shadows can be reduced by increasing the pressing pressure of the probe and the amount of air expelled, the physical burden on the patient also increases. Moreover, because of differences among individuals with respect to the size and positioning of the heart, fat, and lungs, there are significant differences regarding the appropriate probe pressure that could ensure an accurate examination. It is therefore necessary to provide appropriate patient-centric examination conditions. For robotic echocardiography, these parameters must be determined quantitatively, since robots cannot rely on subjective adjustments by physicians. Consequently, this study focuses on identifying fat and lung shadows and developing a method to reduce only the fat shadows in obese patients. Note that this method is applicable to obese males.

II. METHOD

A. Shadow Detection Method

1) Features of Fat and Lung in US Images

To detect both fat and lung shadows, it is necessary to identify the characteristics of these shadows caused by (i) the ultrasonic characteristics of the subcutaneous fat/lungs and (ii) the difference in the positional relationship between the subcutaneous fat/lungs and the heart. For (i), differences in ultrasonic characteristics, such as attenuation coefficient and acoustic impedance, affect the brightness value of the image. For (ii), the positional relationship of each tissue affects the location of artifacts that appear in the image.

The main factors affecting the generation of shadows in (i) are the reflection and absorption of ultrasonic waves. Ultrasonic waves travel straight in a uniform medium; however, when they reach the boundaries of different media, some of the ultrasonic waves are reflected and the rest are refracted and transmitted. The sound pressure reflection coefficient R_p and sound pressure transmission coefficient T_p for an incident ultrasonic wave from medium 1 to medium 2 are expressed by equations (1) and (2), respectively

$$R_I = \frac{Z_2 - Z_1}{Z_2 + Z_1} \quad (1)$$

$$T_I = \frac{2Z_1}{Z_2 + Z_1}, \quad (2)$$

where Z_1 and Z_2 are the acoustic impedances of medium 1 and medium 2, respectively.

When US waves enter the soft tissue from fat, 9.4% of them are reflected and 90.6% are transmitted, due to shadowing caused by subcutaneous fat. Conversely, when the US waves enter the soft tissues from air, then 99.9% of the US waves are reflected and 0.1% are transmitted due to shadows caused by the lungs. The acoustic impedances of air, fat, and human soft tissue (average) were calculated to be 0.00043, 1.35, and $1.63\rho C \times 10^{-6} kg \cdot m^{-2} \cdot s^{-1}$ respectively [18].

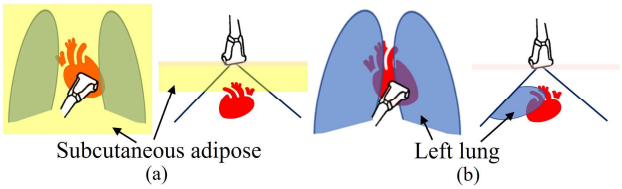

Fig.3. Location of heart, subcutaneous fat and lungs (a) Subcutaneous fat (b) Lungs

The degree of US absorption differs depending on the biological tissue. The degree of absorption is expressed as an attenuation coefficient, which is the ratio of attenuation during the propagation of US waves at 1 cm within a material. The ultrasonic attenuation coefficients of each body tissue are as follows: air: 12.0, fat: 0.6 dB/cm/MHz [18]. This indicates that US waves of 3 MHz used in ultrasonography are attenuated by 18.7% and 98.4%, respectively, when propagating 1.0 cm through fat and air layers. Based on [19], assuming a thickness of 2.5 cm for the adipose tissue layer in obese body types, there is a 40.4% attenuation when passing through the fat layer. Although lung thickness varies with the amount of respiration, most US waves are absorbed even if they pass through only 1 cm of the air layer inside the lungs.

As for (ii), obese males, the subject of this study, do not show any local differences in the thickness of subcutaneous fat in the chest region, which was generally uniformly present (**Fig. 3(a)**). Thus, fat shadows are not anisotropic in the central angular direction of the US image and are considered to occur uniformly from the deepest part of the US image. In contrast, lung artifacts in echocardiography are caused by the presence of air in the left lung, and the position of the artifact is due to the positional relationship between the left lung and the heart. When the heart structure is depicted, the longitudinal direction of the probe passes through the left lung, and the lung area appears from the left side on the US image (**Fig. 3(b)**). Thus, the US image shows anisotropy in the direction of the central angle due to lung shadows, and the image is missing from the left edge.

Based on these features in US images of fat and lungs, the next section proposes distinct methods for detecting fat and lung shadows.

2) Fat Shadow Detection

Although US waves are reflected and absorbed by the fat layer, approximately 60% of them can pass through the fat layer (see Sec. II-A.1). Thus, the fat layer is of medium intensity, and the cardiac structures can be somewhat seen, even though the area deeper than the fat layer is of low luminosity in the US image. Fat thickness ranges from 1.6 mm to 30.1 mm [19]. The proposed method is applied to obese patients, and the fat layer thickness is assumed to be greater than 2.5 mm. The detection algorithm was therefore constructed on the basis of this information, as shown below. Note that the luminance value threshold and distance used in the algorithm were experimentally determined based on the

above information. Furthermore, the algorithm is based on the assumption that the heart component is detected, and it is assumed that this component can be obtained in the fat shadow reduction method described below (see Sec. II-B-2).

(1) The area of luminance value of 20–80 that exists between 2.5 and 5.0 cm in the depth direction is derived.

(2) When a straight line is drawn from the center of the fan-shaped US area in the US image (hereinafter referred to as the US center) to each pixel in the area derived in (1), considering that the maximum luminance value of a pixel whose depth is greater than the depth of the pixel and smaller than 12.5 cm is less than 30, then the area connecting this pixel and the US center is identified as the fat shadow area.

(3) When a fat shadow area is detected in (2), the fat shadow index α_{FO} is calculated from Eq. (3) using the maximum luminance value I_R of the detection area of the acquisition target and the target luminance value I_G that can render the acquisition target clearly.

$$\alpha_{FO} = \frac{I_G - I_R}{I_G}. \quad (3)$$

(4) US images with a fat shadow index α_{FO} of 0.2 or higher are detected as blurred US images due to fat shadows. Note that this threshold was determined visually from the value of the fat shadow index that clearly depicts the heart components when the US images were compared against the fat shadow index, as shown in **Fig. 4**.

US images in which fat shadows are detected using the proposed method are shown in **Fig. 5**.

3) Lung Shadow Detection

The lungs reflect and absorb almost all of the US waves, as discussed in Sec. II-A-1. Thus, the lungs are highly luminous, as opposed to their deeper portions which are less luminous, thereby rendering it difficult to determine the structure of the heart. Considering that the thickness of the lungs varies greatly depending on the volume of air exhaled, an algorithm for lung shadow detection was constructed, as shown below. Note that the luminance values and distance thresholds used in this algorithm were experimentally determined on the basis of the above information.

(1) The area of luminance value of 80–170 that exists between 2.5 and 10.0 cm in the depth direction is derived.

(2) When a straight line is drawn from the US center to each pixel in the area derived in (1), considering that the maximum luminance value of a pixel whose depth is greater than the depth of the pixel and smaller than 12.5 cm is less than 5.0, then the area connecting this pixel and the US center is identified as the candidate lung shadow area.

(3) If the candidate lung shadow area in (2) exists continuously from the left edge of the US area in the US image, this area is considered to be the lung shadow area.

(4) When the lung shadow area is detected in (3), the lung shadow index α_{LO} is calculated from Eq. (4) using the number of pixels in the area of the US image where the lung shadow occurs, P_{LA}, the number of pixels in the area of the US image, P_{EA}, and the correction coefficient C_L. The correction coefficient C_L is set to 100 to match the order of the fat shadow index α_{FO}.

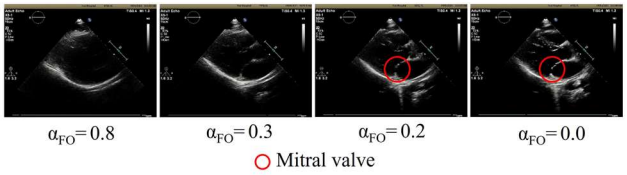

Fig.4. Relationship between fat shadow index and US image clarity

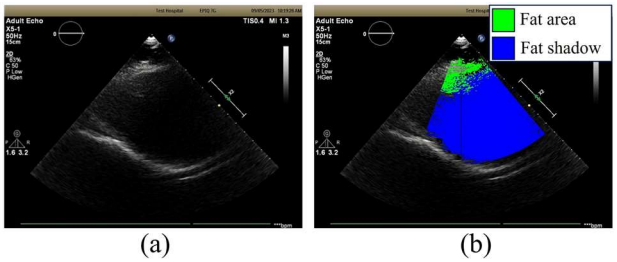

Fig.5. Detection of fat shadows by the fat-shadow detection method (a) Original image (b) Image with fat shadows detected

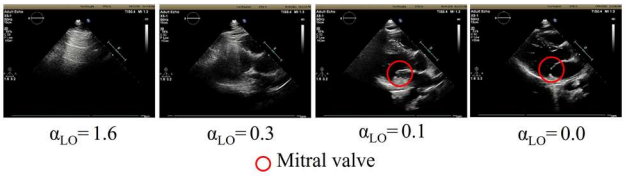

Fig.6. Relationship between lung shadow index and US image clarity

Fig.7. Detection of lung shadows by the lung-shadow detection method (a) Original image (b) Image with lung shadows detected

$$\alpha_{LO} = \frac{C_L \cdot P_{LA}}{P_{EA}}. \quad (4)$$

(5) US images with a lung shadow index α_{LO} of 0.1 or higher are detected as blurred US images due to lung shadows. Note that this threshold was visually determined from the fat shadow index value that clearly depicts the heart structures when the US images were compared against the fat shadow index, as shown in **Fig. 6.**

US images in which lung shadows are detected using the proposed method are shown in **Fig. 7**.

B. shadow Reduction Method

1) Overview

An overview of the shadow reduction method is shown in **Fig. 8**. The fat shadow reduction method improves the clarity of the fat shadow index α_{FO} (see Sec. II-A.2) by adjusting the pressure of the probe. The details of the method are described in the following sections. The patient's posture is represented by θ_{roll} and θ_{pitch}, where θ_{roll} is defined as 90^0 minus the angle formed between the gravity vector and the frontal axis of the body, and θ_{pitch} is defined as 90^0 minus the angle between the gravity vector and the sagittal axis of the body.

2) Fat Shadow Reduction

In medical practice, the probe is pressed hard against the patient's body to compress the fat layer between the probe and the heart, thereby reducing fat shadows. In contrast, the adjustment of probe pressure during this process is performed subjectively by the physician, and the appropriate probe pressure remains unknown. Thus, in this section, we propose (i) a probe pressure adjustment mechanism that enables the echocardiography robot to adjust the probe pressure and (ii) a visual servo method to reduce fat shadows based on the results of our preliminary tests to identify the appropriate probe pressure.

An overview of (i), which presents the probe pressing pressure adjustment mechanism, is shown in **Fig. 9**. This mechanism uses a slider (EASM4XE015AZMC, Oriental Motor, Japan), load cell (LSMS-20K, MinebeaMitsumi, Japan), indicator (CSD-701B, MinebeaMitsumi, Japan), and spring (VUL4-30, MISUMI, Japan). As shown in **Fig. 9(a)**, the balance of the forces of the units composing the mechanism results in the pressing force of the probe on the patient's body being equal to the force applied to the two load cells and the elastic force of the three springs. Thus, the pressing force of the probe can be measured as the sum of the forces applied to the two load cells. As shown in **Fig. 9(b)**, when the slider is moved up and down, the spring part expands and contracts, respectively, thereby allowing the probe pressing force to be increased or decreased accordingly. By combining these two functions, the probe pressing pressure can be adjusted to the target value.

Next, a preliminary test was conducted on (ii) to identify the appropriate probe pressing pressure. The subjects for the preliminary test were 9 obese males in their twenties. (BMI: 30.5 ± 5.0) and six normal-sized males (BMI: 22.7 ± 2.4). The details of the preliminary study are shown below. Among the heart components, the present study evaluated the mitral valve.

(1) The subject was placed on the echocardiography robot, and the probe was moved to a position where the mitral valve could be clearly acquired.

(2) The probe force was varied from 0.0 to 10.0 N, and US images were acquired.

(3) The mitral valve was detected by machine learning (YOLOv7[20]) from the acquired images, and the probe force was obtained when the mitral valve was detected.

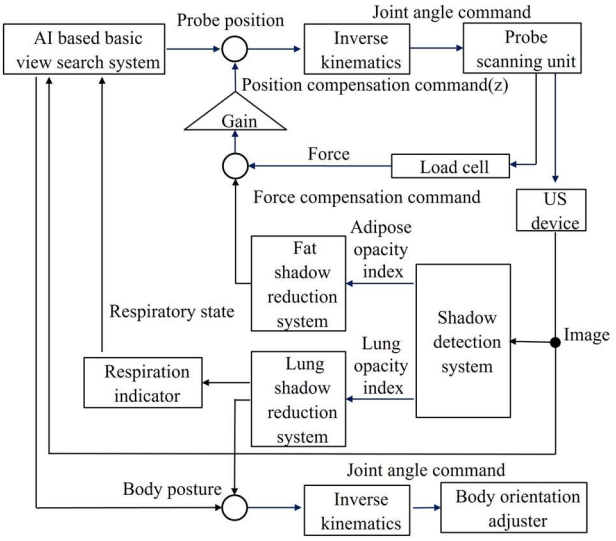

Fig.8. Overview of shadow reduction method

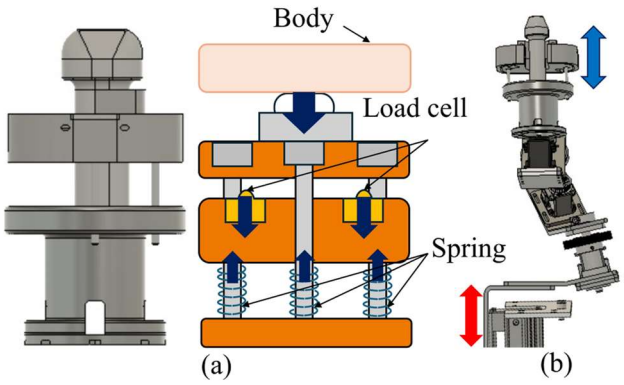

Fig.9. Probe force adjustment mechanism (a) Measuring section (b) Pressurizing and depressurizing section

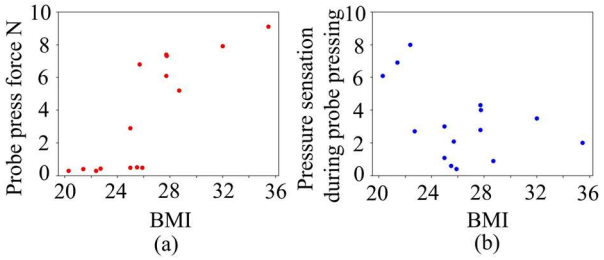

Fig.10. Relationship between obese patients and probe pressure (a) Relationship between BMI of the patient and the probe pressure at which the mitral valve can be observed (b) Relationship between BMI of the patient and the pressure sensation when pressing the probe

(4) The subjects were asked to complete a 10-point Visual Analog Scale (VAS) questionnaire regarding the pressure sensation caused by the probe when a 10.0 N probe force was applied.

(5) Based on the results of (3) and (4), the appropriate probe pressing pressure was derived, which would in turn enable the clear acquisition of the heart components, and which would not cause any pressure sensation in the patient.

Fig. 10(a) shows the relationship between the subjects' BMI and the probe force that could accurately detect the mitral valve. In addition, **Fig. 10(b)** shows the relationship between the VAS evaluation of each body type and pressure sensation when a probe force of 10.0 N was applied. Our findings revealed that there was a strong positive correlation ($r = 0.83$) between the probe force that could detect the mitral valve and the subjects' BMI. In contrast, there was a moderate negative correlation ($r = -0.45$) between patients' BMI and the probe force.

The results showed that it was necessary to increase the probe pressing force with increasing value of BMI to clearly acquire the heart components; however, at the same time, it was difficult to feel the pressure sensation even when the probe pressing force was increased. This might be because the pressing pressure of the probe compresses the body organs when the BMI is low and the fat layer is thin, whereas in patients with high BMI, whose fat layer is thick, the fat layer acts as a cushion, absorbing the pressing pressure of the probe and avoiding any compression to the body organs. This indicates that the fat shadow can be reduced without pressure sensation by compressing the fat layer with appropriate probe pressure according to the patients' BMI.

In contrast, it is thought that the patient is bound to feel a sense of pressure when the force applied to the probe is more than the appropriate. Thus, if the probe is pressed down until it reduces the fat shadow on the entire US image acquired, the pressing pressure applied to the probe is likely to be excessive, resulting in a feeling of pressure. Then, scanning is performed with a feed-forward control, which shows the minimum pressing pressure at which the heart structure deep in the fat layer can be determined according to the individual's BMI. Once the area of the heart that is to be observed is identified, feedback control is performed to adjust the probe pressure and improve the clarity of that area. A combination of these two methods is proposed to reduce fat shadows, enabling the reduction of fat shadows and minimizing pressure sensation. The details of the proposed method are described below.

(1) The initial value of the probe pressure, F_p [N], is calculated from Eq. (5), and scanning is initiated. If F_p is less than 0.5 N, then F_p should be set to 0.5 N. Note that B_p is the BMI of the patient.

$$F_p = 0.721 \times B_p - 15.2 \quad (5)$$

(2) When the specific area of the heart is detected, fat shadow detection proposed in Sec. II-A.2, is performed to evaluate whether fat shadows are generated or not.

(3) When fat shadows are detected, the probe pressure is increased to reduce the fat shadows. In the absence of fat shadows, the initial probe pressing pressure indicated in (1) should be used and the run should be continued.

III. Evaluation

A. Experimental Setup

The shadow detection method and the shadow reduction method were subsequently tested using a seated echocardiographic robot [16], a matrix array sector probe (X5-1, Philips, The Netherlands), and a US system (EPIQ 7G, Philips, The Netherlands).

1) Shadow Detection Method Validation

The purpose of this experiment was to evaluate the accuracy of the proposed shadow detection method and confirm its validity. Nine obese males in their twenties (BMI: 30.3 ± 5.3) were included, and the details of the test are shown below.

(1) The subject was placed on the echocardiography robot, and the probe was moved to a position where the mitral valve could be clearly observed.

(2) The subject was brought to the resting expiratory level, and the probe pressing force was increased or decreased in the range of 0.0–10.0 N. The US images acquired at that time were acquired as candidate images in which fat shadows were generated.

(3) The US images acquired while the subject exhaled from the maximal inspiratory level to the maximal expiratory level were acquired as a group of candidate images in which lung shadows were generated.

(4) The candidate images in which fat shadows occurred (Step (2)) were divided into images in which fat shadows occurred and images in which no shadows occurred.

(5) The candidate images with lung shadows acquired in Step (3) were divided into images with and without lung shadows.

(6) The proposed shadow detection method was applied to a group of images with fat shadows, lung shadows, and no shadows. The recall rate, precision rate, and F-measure were calculated for the classification accuracy of each image group. The validity of the proposed shadow detection method was verified on the basis of these values. Note that for the group of images in which no shadows were generated, the classification was considered successful in the absence of both fat and lung shadows when the proposed shadow detection method is implemented.

2) Shadow Reduction Method Validation

The experiment confirmed the validity of the proposed shadow reduction method. Two males in their twenties (both with a BMI of 25.7, hereafter referred to as subjects A and B) were included, and the details of this study are as follows.

(1) The subject was placed on the echocardiography robot, and his xiphoid process was aligned with the initial position of the probe. Note that the method for respiratory instructions and posture was determined based on our previous study [21].

(2) The probe position (x-axis and y-axis) was moved, and the left chest wall was scanned in a five-way traveling manner. The mitral valve was detected by machine learning (YOLOv7[20]) on US images obtained at that time. The roll,

TABLE I. ACCURACY OF SHADOW DETECTION METHOD

	Recall %	Precision %	F-measure %
Adipose opacity	100.0	86.4	92.7
Lung opacity	95.1	98.5	96.8
No opacity	93.5	100.0	96.6

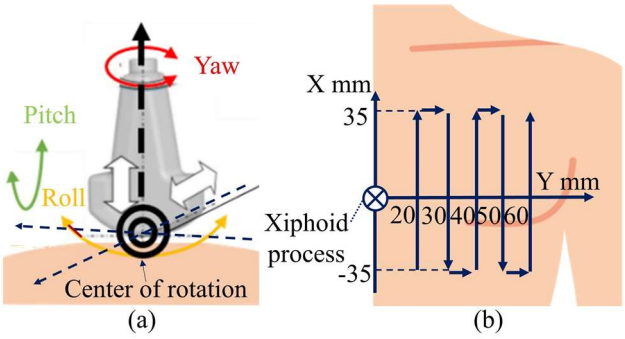

Fig.11. Degrees of freedom and trajectory of the probe (a) Degrees of freedom of the probe (b) Trajectory of the probe

pitch, and yaw of the probe were then defined, as shown in **Fig. 11(a)**, and were set to 0° for the five-way traveling scan. (3) Step (2) was performed six times for each condition, with and without the shadow reduction method. As for the range of application of the lung shadow reduction method in the patient's chest area, Step (2) was performed on each subject in the initial posture as a preliminary test, and the range in which the mitral valve could be obtained was visually confirmed and the range of application was determined. (4) The number and range of mitral valve detections with and without the shadow reduction method were derived. Then, the validity of the proposed shadow reduction method was verified by comparing the above results.

B. Results

1) Shadow Detection Method Validation

Table 1 shows the recall, precision, and F-measure of the proposed shadow detection method for US images with fat shadows, lung shadows, and no shadows. For evaluation, ground truth labels for fat and lung shadows were manually annotated by the researchers based on visual inspection of the ultrasound images.

2) Shadow Reduction Method Validation

The number and range of mitral valve detections with and without the shadow detection and reduction method for subjects A and B are shown in **Fig. 12.** and **Fig.13**, respectively. Statistical analysis of the number of mitral valve detections was performed using the Wilcoxon signed-rank sum test. A significant tendency was found between the

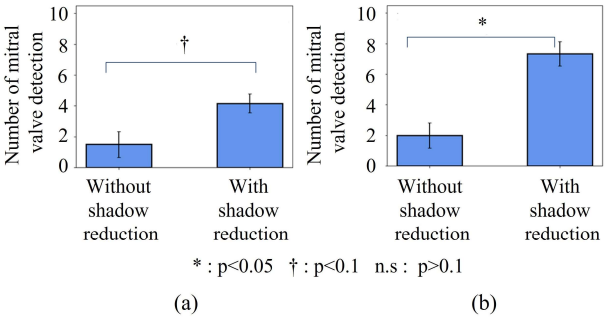

Fig.12. Number of mitral valve detections with and without shadow reduction (a) Subject A (b) Subject B

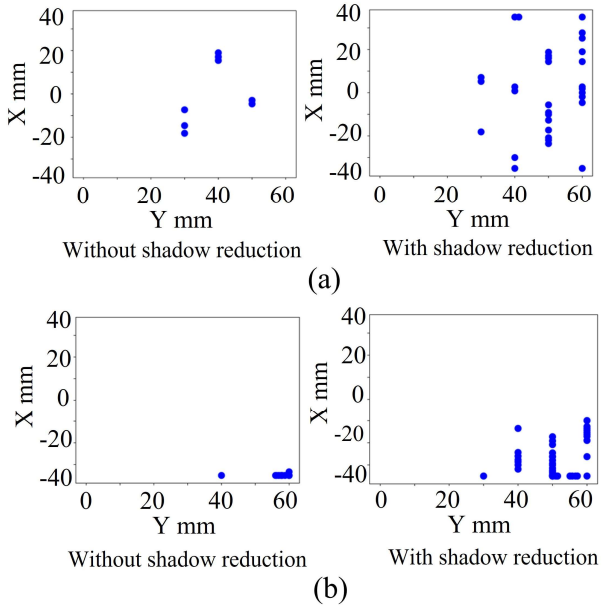

Fig.13. Detection area of mitral valve with and without shadow reduction (a) Subject A (b) Subject B

conventional and proposed methods for subject A (p = 0.0625), and a significant difference was found between the conventional and proposed methods for subject B (p = 0.0313).

C. Discussions

1) Shadow Detection Method Validation

Our results suggest that the proposed method can classify shadows with high accuracy. However, false negative or false positive results may occur when classification is based only on information from a single US image. This issue can be mitigated by determining whether a shadow is present based on the detection results of the target US image and those of the US images acquired before and after it.

With respect to patient safety, we did not move the probe at a high speed (approximately 10.0 mm/s) during the echographic examination. Fat shadows tend to occur continuously with respect to the probe position because they are continuously present in the human body. In addition, the US images are acquired at approximately 30 Hz. From the

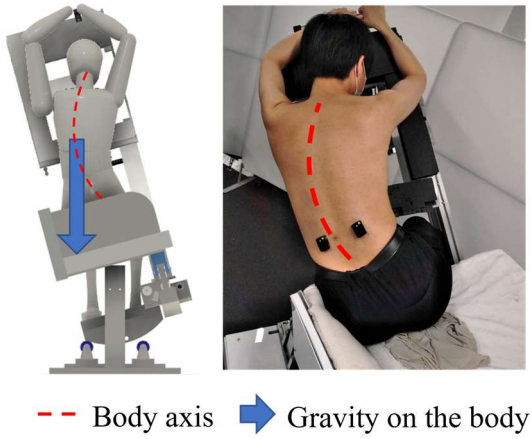

Fig.14. Subjects on the echocardiography robot during body bending (a) Model (b) Actual passenger

above, it is highly likely that the same type of shadows occurs in the US images before and after the US image for which detection is performed. By classifying shadows based on the detection results of multiple images, including pre- and post-US images, the proposed shadow detection method is expected to have a higher accuracy.

2) Shadow Reduction Method Validation

The results showed that the proposed method could not only reduce the shadows but also enable the detection of mitral valves in a wide area for subjects A and B, thereby validating the effectiveness of the proposed method. However, when the proposed method was applied, the number of mitral valve detections was lower for subject A than for subject B, and the statistical results of the proposed method against the conventional method for subject A remained in a significant trend.

This is thought to be because the subject's posture becomes less stable when the echocardiography robot used in this study bends the subject's body sideways than when the subject is not bending. When the echocardiography robot bends the subject to the side, the subject is subjected to a rotational moment generated by the body's center of gravity, which causes the body axis to bend (**Fig. 14**). Moreover, the echocardiography robot is less constrained to the subject to ensure emergency evacuation. The subject's body is considered to move more easily to adjust their body position when subjected to a body load due to the rotational moment caused by the body's center of gravity, in order to alleviate that body load.

In case of a bent body axis, there is a misalignment between the body and the part of the inspection device that moves the probe, making it impossible to scan over the necessary area for inspection. In case the subject has moved due to adjustment of the subject's body position, the subject's body moves during the examination, making it difficult to maintain the appropriate probe pressure and possibly resulting in incomplete reduction of fat shadows. These problems can be solved in the future by developing a robotic mechanism that counteracts and supports the rotational moment caused by the subject's center of gravity during lateral bending. Also, the introduction of a probe pressing mechanism with high responsiveness to the subject's body misalignments can be very helpful.

D. Limitations

There are several limitations to the proposed method and verification method. First, the proposed method is limited to male subjects, and the number of subjects was limited. In females, fat distribution varies significantly, primarily due to the fat present in breasts, and it is therefore necessary to adjust the breast position and provide appropriate probe pressure in the medical field. Based on the relationship between fat and probe pressure confirmed by this method, it is necessary to propose an examination method in the future that can be applied to females using an echocardiography robot.

Second, the thresholds for shadow presence or absence were determined based on visual inspection using the fat shadow index and lung shadow index defined in Sec. II-A.2 and Sec. II-A.3, respectively. However, it is unclear whether this criterion is medically suitable for diagnosis. In the future, it will be necessary to collaborate with physicians to define clear diagnostic criteria for the fat shadow index and lung shadow index.

IV. Conclusion

The main issue with robotic echocardiography is that it is challenging to obtain clear US images in obese patients due to lung and fat shadows. In this study, a method for detecting fat and lung shadows and reducing fat shadows was proposed to improve US image acquisition in obese patients. Preliminary experiments on the fat shadow reduction method showed that as the patient's BMI increases, the probe force needs to be increased to obtain clear images of the cardiac structures. At the same time, patients are less likely to feel pressure even when the probe force is increased. Based on these results, we derived an appropriate probe pressure for the patient's BMI and proposed a mechanism for presenting that pressure, thereby rendering the acquisition of US images possible without the patient feeling pressure and with minimal fat shadows. A validation test of the proposed method was conducted. The proposed method was able to detect fat and lung shadows with F-measures of 92.7% and 96.8%, respectively, thereby confirming the usefulness of the shadow identification method. The shadow reduction method increased the number of mitral valve detections and expanded the range of mitral valve detection, suggesting the usefulness of the shadow reduction method. Future work will involve validation of the proposed method on a larger and more diverse patient population and integration with automatic acquisition of standard echocardiographic views to enable

robotic acquisition of diagnostic cross-sections in obese patients.

ACKNOWLEDGMENT

This research was supported by the NSK Foundation for Advancement of Mechatronics and the Institute for Mechanical Engineering Frontiers.

REFERENCES

[1] WHO (World Health Organization), "Cardiovascular diseases (CVDs)," 2021, https://www.who.int/news-room/fact-sheets/detail/cardiovascular-diseases-(cvds), Accessed 30 January 2023

[2] C. W. Yancy, M. Jessup, B. Bozkurt et al. 2013 ACCF/AHA guideline for the management of heart failure: executive summary: a report of the American College of Cardiology Foundation/American Heart Association Task Force on practice guidelines. Circulation, vol. 128, no. 16, pp. 1810-1852, 2013.

[3] N. Koizumi, S. Warisawa, M. Nagoshi, H. Hashizume, and M. Mitsuishi, "Construction methodology for a remote ultrasound diagnostic system," IEEE Trans. Robot., vol. 25, no. 3, pp. 522–538, 2009.

[4] P. Abolmaesumi, S. E. Salcudean, W. H. Zhu, M. R. Sirouspour, and S. P. DiMaio, "Image-guided control of a robot for medical ultrasound," IEEE Trans. Robot. Autom., vol. 18, no. 1, pp. 11–23, 2002.

[5] K. Ito, S. Sugano, and H. Iwata, "Portable and attachable tele-echography robot system: FASTele," 2010 Annu. Int. Conf. IEEE Eng. Med. Biol. Soc. EMBC'10, pp. 487–490, 2010.

[6] A.S.B. Mustafa, T. Ishii, Y. Matsunaga, R. Nakadate, H. Ishii, K. Ogawa, A. Saito, M. Sugawara, K. Niki, and A. Takanishi, "Development of robotic system for autonomous liver screening using ultrasound scanning device," IEEE Int. Conf. Robot. Biomimetics, pp. 804–809, 2013.

[7] T. Y. Fang, H. K. Zhang, R. Finocchi, et al, "Force-assisted ultrasound imaging system through dual force sensing and admittance robot control," Int. J. Comput. Assist. Radiol. Surg., vol. 12, no. 6, pp. 983–991, 2017.

[8] P. Arbeille, J. Ruiz, P. Herve, M. Chevillot, G. Poisson, and F. Perrotin, "Fetal tele-echography using a robotic arm and a satellite link," Ultrasound Obstet. Gynecol., vol. 26, no. 3, pp. 221–226, 2005.

[9] J. Esteban, W. Simson, S. R. Witzig, A. Rienmüller, S. Virga, B. Frisch, O. Zettinig, D. Sakara, Y. Ryang, N. Navab and C. Hennersperger., "Robotic ultrasound-guided facet joint insertion," Int. J. Comput. Assist. Radiol. Surg.,vol. 13, no. 6, pp. 895–904, 2018.

[10] S. Wang, D. Singh, D. Johnson, K. Althoefer, "Robotic Ultrasound: View Planning, Tracking, and Automatic Acquisition of Transesophageal Echocardiography," IEEE Robot. Autom. Mag., vol. 23, no. 4, pp. 118–127, 2016.

[11] R. Tsumura, J. W. Hardin, K. Bimbraw, et al, "Tele-Operative Low-Cost Robotic Lung Ultrasound Scanning Platform for Triage of COVID-19 Patients," IEEE Robotics and Automation Letters, vol. 6, issue. 3, pp. 4664–4671, 2021

[12] R. Tsumura and H. Iwata, "Robotic fetal ultrasonography platform with a passive scan mechanism," International Journal of Computer Assisted Radiology and Surgery, vol. 15, pp. 1323–1333, 2020.

[13] Y. Shida, R. Tsumura, T. Watanabe and H. Iwata, "Heart Position Estimation based on Bone Distribution toward Autonomous Robotic Fetal Ultrasonography,"2021 IEEE International Conference on Robotics and Automation, paper no.940, 2021

[14] Y. Takachi, K. Masuda, T. Yoshinaga et al, "Development of a Support System for Handling Ultrasound Probe to Alleviate Fatigue of Physician by Introducing a Coordinated Motion with robot,", Journal of the Robotics Society of Japan, vol. 29, no. 7, pp.634–642, 2011.

[15] M. Giuliani, D. Szczęśniak-Stańczyk, N. Mirnig, et al "User-centred design and evaluation of a tele-operated echocardiography robot", Health and Technology, vol. 10, pp.649-665, 2020

[16] Y. Shida, M. Sugawara, R. Tsumura, et al, "Diagnostic Posture Control System for Seated-Style Echocardiography Robot," International Journal of Computer Assisted Radiology and Surgery, vol 18, issue. 3, 2023

[17] Y.Shida, S. Kumagai, R. Tsumura et al, "Automated image acquisition of parasternal long-axis view with robotic echocardiography." IEEE Robotics and Automation Letters, vol. 8, no. 8, pp. 5228-5235, 2023

[18] B.B. Goldberg, P.N.T.Wells, "Ultrasonics in clinical diagnosis, Edinburgh", Churchill Livingstone, 1977.

[19] P. Störchle, W. Müller, M. Sengeis. et al. "Measurement of mean subcutaneous fat thickness: eight standardised ultrasound sites compared to 216 randomly selected sites." Sci Rep 8, 16268, 2018

[20] C. Y. Wang, A. Bochkovskiy, H. Y. M. Liao, "YOLOv7: Trainable bag-of-freebies sets new state-of-the-art for real-time object detectors," arXiv, 2022.

[21] T. Hashimoto, Y. Shida. S. Kumagai, et al, "Development of a seated echocardiography robot - lung volume and body posture conditions that enable clear mitral valve echocardiographic images – ", 2023 IEEE/SICE International Symposium on System Integration,2023.